Micro-Raman Investigations of the Formaldehyde−Ice System

ARTICLE *in* THE JOURNAL OF PHYSICAL CHEMISTRY B · FEBRUARY 2005

Impact Factor: 3.3 · DOI: 10.1021/jp040244w · Source: PubMed

Micro-Raman Investigations of the Formaldehyde−Ice System

Bertrand Chazallon,*† Nathalie Lebrun,‡ Paul Dhamelincourt,§ Céline Toubin,† and Cristian Focsa†

Laboratoire de Physique des Lasers, Atomes et Molécules (UMR 8523), Centre d'Etudes et de Recherches Lasers et Applications (CERLA), Université des Sciences et Technologies de Lille, 59655 Villeneuve d'Ascq Cedex, France, Laboratoire de Dynamique et Structure des Matériaux Moléculaires (UMR 8024), Université des Sciences et Technologies de Lille, 59655 Villeneuve d'Ascq Cedex, France, and Laboratoire de Spectrochimie Infrarouge et Raman, Centre d'Etudes et de Recherches Lasers et Applications (CERLA), Université Lille 1, 59655 Villeneuve d'Ascq, France

Received: March 25, 2004; In Final Form: August 4, 2004

Rapidly frozen aqueous solutions containing variable amounts of dissolved formaldehyde (0.1, 5, 7, 10, 15, and 20 mol %) have been analyzed by micro-Raman spectroscopy at ambient pressure and low temperature. The importance of the formladehyde−ice system has been repeatedly quoted in various contexts, such as atmospheric and snowpack chemistry and interstellar and cometary ices. Understanding and characterizing the effects of freezing and the interactions of formaldehyde with ice are therefore of relevant interest. In this study, the distinct vibrational signatures of the oligomers present in the solution and in the frozen ice mixtures have been identified in the 120−4000 cm^{-1} spectral range. From the subtle changes of the bands assigned to the CO and CH group frequencies, at least two distinct crystalline phases (pI and pII) are found to coexist with ice at different temperatures. Depending on the cooling−rewarming protocol, pI is found to crystallize in the 163−213 K temperature range. Above ∼213 K, pI gets transformed irreversibly into pII which is stable up to ∼234 K. pII is found to interact more strongly with ice than pI, as revealed, for example, by the drop in frequency of the bands assigned to the O−H stretching as pI transforms into pII. It is suggested that pII consists of a hydrogen-bonded network of oligomers and water molecules. On the other hand, it is suggested that the oligomers mainly present in pI interact through weak forces with the surrounding water molecules.

I. Introduction

The formaldehyde−ice system is known to play an important role in atmospheric and snowpack chemistry.[1] This is illustrated by its contribution to the production of HO_x radicals, which largely determine the lifetime of trace gases (e.g. pollutants) in the atmosphere. Formaldehyde (H_2CO) can also be an important sink for free radicals, such as Br atoms that catalyze ozone destruction in the Arctic boundary layer.[2] However, the activation of bromine and the contribution of H_2CO in the oxidation of halides and molecular halogens are not fully understood.[3] Formaldehyde has also proven to have a strong influence on the global mixing rate of ozone and OH radicals, which govern the oxidizing capacity of the troposphere.[4,5] As a consequence, H_2CO present in the polar ice core potentially provides valuable data on past oxidizing capacity of the atmosphere.[6]

Importance of the formaldehyde−ice system has also been revealed in the extraterrestrial environment since poly(oxymethylene) (POM), which is a H_2CO polymerization product ($-(H_2CO)_n-$), was the first polymer identified in space.[7,8] Previous investigations involving formaldehyde and ice were mostly focused on reaction products of multicomponent gas condensed-ice mixtures. Furthermore, these studies reported the influence of combined processes that include gas grain chemical reactions and irradiation (UV or cosmic-ray bombardment) in the astrophysical context. Although H_2CO is known to be present as trace concentrations in polluted or unpolluted rural areas (∼0.1 to 100 ppbv[4,9]), its concentration reaches the percent level relative to H_2O (the dominant species) in icy mixtures of cometary nuclei[10] or in interstellar ice.[11] Reactions of gas condensed formaldehyde with ice (e.g., $H_2O + H_2CO + CH_3OH + NH_3 + CO$) have been studied extensively,[12−14] under irradiation or by thermal excitation. Schutte et al.[12] have demonstrated the ability to produce different complexes of organic materials (e.g., POM), depending on the relative amounts of the different components of the ice mixture and on the excitation process involved. Although polymerization of H_2CO may in this case be initiated by unusual processes (irradiation, thermal activation, chemical reactions) and may result from solid reorganization at low temperature (<100 K),[12] formaldehyde is known to polymerize readily in water solutions to form POM glycols ($HO(H_2CO)_nH$). Thereby, the abundance of high oligomers (large *n* values) increases with the concentration of dissolved H_2CO.[15,16] Because of the difficulty in producing monomeric formaldehyde due to its high instability in the gaseous state,[17] formaldehyde is, thus, usually produced in aqueous solutions or in liquid polymerized form for industrial applications.[18] On the other hand, it turns out that the cooling of such solutions below 283 K may induce polymerization.[18]

To our knowledge, no spectroscopic data have been reported on this system at temperatures below freezing, nor has it ever been thoroughly characterized. For these reasons, an improvement of our understanding of the formaldehyde−water interac-

* To whom correspondence should be addressed. Phone: +33 (0)320336468. Fax: +33 (0)320336463. E-mail: chazallon@phlam.univ-lille1.fr.

† Laboratoire de Physique des Lasers, Atomes et Molécules.

‡ Laboratoire de Dynamique et Structure des Matériaux Moléculaires.

§ Laboratoire de Spectrochimie Infrarouge et Raman.

10.1021/jp040244w CCC: $30.25
Published on Web 12/09/2004

tions at temperatures below freezing appears especially useful. It is, furthermore, illustrated by the contribution of this system in cryobiological and biophysical context. Indeed, formaldehyde may exhibit the required properties of a good cryoprotector compound.[19] Although the mechanism and origin of the action of protective additives at the molecular level against freezing damage of living systems are still obscure,[20] it has been found that the protective action of polymers may be due to a number of factors.[21] Of main interest is the ability of a cryoprotector upon freezing to preserve hydrogen bonds within the solvent; i.e., the fact that the amount of free water molecules within a biological cell reduces during the ice growth. This should prevent a substantial fraction of water molecules from freezing. A cryoprotector should also hamper the formation of large ice crystals, which are likely to enlarge during warming and, thus, may damage the cell membrane and make cells leaky.[22] Another property is the reduction of the melting temperature of the water−cryoprotector eutectic by maintaining a relatively high molecular mobility at low temperatures; this will keep the biological fluids or cellular cytoplasm in the liquid state at lower temperature. Even though formaldehyde and its oligomers are not yet of cryomedical importance, our understanding of the formaldehyde−ice system could be regarded as model studies for future applications of cryoprotection.

Attempts have been made previously to determine the effects of freezing on the water−formaldehyde system in concentrated mixtures (40% H_2CO).[23] Presence of long chain clusters ($-(H_2CO)_p-$) and mixed clusters ($-(H_2CO)_p(H_2O)_n-$) has been determined by infrared laser desorption[24] or fast atom bombardment.[23] In this latter work, cluster series have been tentatively related to the presence of a liquid crystalline state in frozen formaldehyde solution at a temperature close to that of liquid nitrogen. Moreover, it was suggested that POM or POM derivatives form a solid make-up of oligomers that interact through weak van der Waals forces due to the absence of an H-bonded network. However, no direct evidence for the presence of a liquid state at low temperature has so far been established by nondestructive microprobing techniques.

To get better insights on the effects of freezing on the water−formaldehyde system and to obtain related information on the ice−formaldehyde interactions, we have undertaken a series of experiments on frozen formaldehyde aqueous solutions. The temperature behavior of the frozen solids is analyzed in situ by micro-Raman spectroscopy at ambient pressure and low temperature.

II. Experimental Methods

Aqueous solutions of different concentrations (0.1, 5, 7, 10, 15, 20 mol % H_2CO) are first prepared according to the procedure described in a previous paper.[16] Methanol is often added as a stabilizer in concentrated solutions. In our case, special care is taken to prepare methanol-free solutions in order to record Raman spectra without spectral interference from methanol or hemiacetal. One droplet (diameter of ∼2 to 3 mm) of H_2CO solution is deposited onto a small metal crucible placed into a LINKAM TMS600 heating/freezing stage. The stage temperature is controlled with a precision of ±1 K and regulated with a nitrogen gas flow as refrigerant. The liquid droplet is maintained at room temperature before being rapidly cooled to 228 K in ∼90 s to initiate crystallization. A subsequent cooling to 163 K is performed to complete the crystallization (see below). However, even for the lowest H_2CO concentrations (0.1 mol %), freezing of the entire solution could only be completed upon rewarming at ∼203 K, in accordance with previous observations of rapidly quenched formaldehyde solutions.[19] The temperature is then increased up to the ambient in different steps with 10 K increments until a complete melting of the frozen solid is achieved.

The Raman spectra are recorded with the help of a LABRAM microRaman spectrometer (Jobin Yvon) equipped with an Olympus microscope (BX-40) on which the LINKAM stage is mounted. The excitation radiation ($\lambda = 632.8$ nm) is produced by an internal He−Ne laser source. The scattered light is analyzed by using a single monochromator spectrograph equipped with a 1800 lines/mm grating and a liquid-nitrogen-cooled CCD detector. A 200-μm entrance slit was typically used, giving a 7 cm^{-1} mean spectral resolution. The laser power at the sample through the cell double windows (trisilicate glass) is ∼5 mW. These windows are fixed onto the cell's lid by a locking ring and separated from each other by two silicon rubber rings. The circular beam spot size has a diameter of ∼2 μm when using a ULWD Olympus ×50 objective (0.6 numerical aperture, 7-mm working distance). The system works in a confocal configuration, allowing nearly the total elimination of the contribution of the out-of-focus zones. More than 250 spectra were collected and were baseline-corrected. The peak positions were established using a least-squares fitting procedure.

III. Results

A. Temperature-Induced Crystallization Observed by Optical Microscopy. In Figure 1, typical aspects of the frozen mixture surface are shown for different temperatures and for different concentrations: 5, 10, and 15 mol % of H_2CO dissolved in water. It is worth noting that for all the concentrations, the same general behavior with temperature is observed. Three steps in relation with the formation of different solid phases are presented. In step (a) (Figure 1), a homogeneous opaque surface appears during freezing at ∼228 K. This corresponds to the crystallization of ice, since water is the major component in the aqueous solutions. At this stage, our Raman analysis reveals the presence of a liquid state that coexists with ice. It is presumably composed of water and short oligomers (see below). Further cooling to 163 K increases slightly the opacity of the sample. Relatively low rates of cooling, such as those chosen in our experiments, lead generally to samples with an opaque appearance. This can be explained by the continuous growth of ice during freezing, which leads to the formation of randomly oriented grains of various sizes and shapes. On the other hand, transparent solids may be obtained when aqueous solutions are quenched with a sufficiently rapid rate of cooling to limit the amount of ice formed (∼300 K/s).[19,25] As the temperature increases from 163 to 213 K in step (b) (Figure 1), the surface changes and becomes slightly mottled at 213 K with a rough-looking appearance, as compared to the smooth surface of step (a). These changes are here related to the formation of a solid phase (pI) in coexistence with ice, as revealed by our Raman analysis (see below). This phenomenon is observed for all of the three solutions. Further heating (step (c), Figure 1) results in a significant change of the surface at ∼223 K with increasing amounts of rodlike forms and thin dark patches. According to our Raman analysis (see below), this stage has been associated with the presence of ice and a distinct solid phase (pII). Above ∼234 K (step (d), Figure 1) a smooth surface appears again, suggesting the presence of ice and the liquid phase previously encountered in step (a). Further heating results in the melting of the complete sample at different temperatures according to the dissolved H_2CO concentration.

B. Temperature-Induced Crystallization Observed by Micro-Raman Spectroscopy. Figure 2 displays Raman spectra

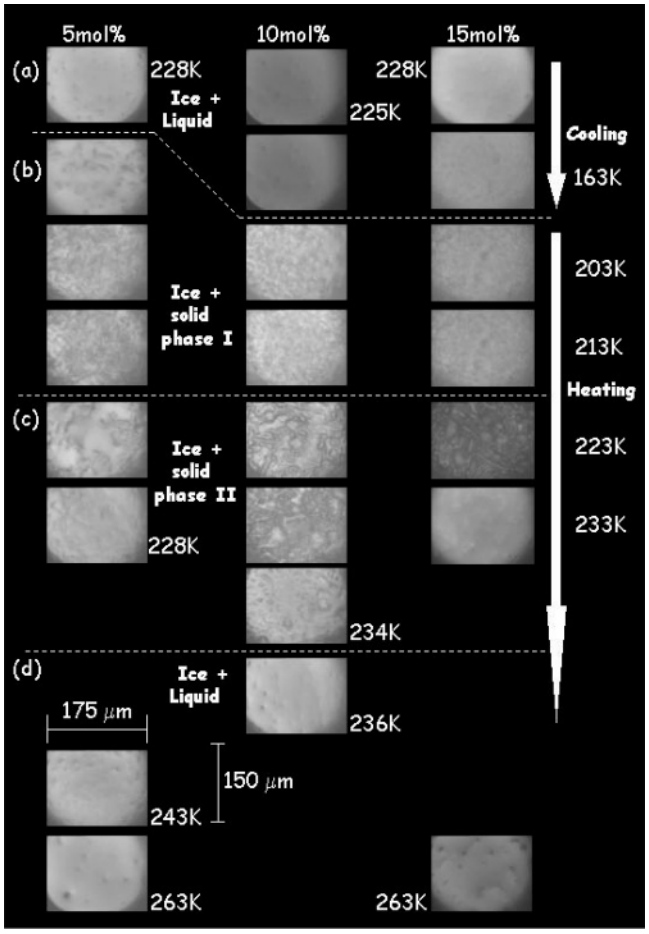

Figure 1. Typical microphotographs of the temperature evolution of frozen formaldehyde−water solutions at different concentrations. (a) Pictures of surface in reflected light of different liquid droplets containing 5, 10, and 15 mol % H_2CO in water after freezing at 228, 225, and 228 K, respectively. This step corresponds to the crystallization of ice surrounded by a liquid mixture (see text). (b) Heating between 163 and 213 K: the sample surface becomes slightly mottled until 213 K and darkens; this step reveals the formation of the pI phase, which coexists with ice (see text). (c) Heating between 213 and 234 K: a large number of very thin dark patches are observed at 223 K. This step corresponds to the formation of pII in coexistence with ice (see text). (d) Heating between 234 and 263 K: the surface regains its smooth aspect as in (a), in which only ice and a liquid mixture are observed.

of a 10 mol % H_2CO−ice mixture in the 120−3700 cm^{-1} frequency range at different temperatures. It is known that a 10 mol % H_2CO aqueous solution contains oligomers in various abundance: ∼68% of them are methylene glycol, whereas only ∼28% of them are dioxymethylene glycol.[15] Each spectrum coincides to a microscopic observation previously made for a given temperature (Figure 1). A notably better signal-to-noise ratio is obtained when increasing the solute concentration. The experimental frequencies from a 10 mol % H_2CO−ice mixture and an aqueous formaldehyde solution of the same concentration are reported in Table 1. Experimental and calculated frequencies for solid POM (paraformaldehyde) are also listed. Presence of ice is clearly identified during cooling at 233 K (Figure 2), partly because of the presence of two bands located at ∼220 and ∼300 cm^{-1}, which correspond to the ice translational lattice modes.[26] On the spectrum recorded at 233 K, broad bands are observed at ∼920 and ∼1050 cm^{-1}, at the same frequencies as those observed in the spectrum of the aqueous solutions recorded at room temperature. This means that a residual liquid (or at least an amorphous state) is still present at 233 K. This residual liquid is presumably composed of noncrystallized oligomers (methylene glycol + dioxymethylene glycol) and water molecules.

As expected, as the ice crystallizes, the broad band corresponding to the O−H stretching for the liquid water is downshifted to give a prominent sharp band at ∼3130 cm^{-1} (υ_s) with a ∼125 cm^{-1} bandwidth (fwhm). This band is generally observed at 163 K, once the ice growth process is well-established.

Upon rewarming from 163 to 203 K, the 10 mol % oligomer mixture starts to crystallize, as indicated by the emergence of sharp bands in different spectral regions at ∼545, ∼575, ∼930, and ∼1036 cm^{-1}, corresponding to CO vibrational modes, and at ∼1241, ∼1275, ∼1314, ∼1409, ∼1487, and ∼1498 cm^{-1}, corresponding to CH vibrational modes. The crystallization of pI is almost entirely completed as the temperature rises up to 213 K.

The spectra recorded at 218, 220, and 223 K show a marked difference with the one at 213 K. This is consistent with the microscopic observation displayed in Figure 1 and the presence of phase pII. Between 218 and 223 K, incomplete crystallization may still occur and is characterized by the coexistence of a residual liquid or amorphous component with ice and pII. In most cases, this liquid is heterogeneously dispersed on the sample surface. During heating from 213 to 218 K, some bands of the O−C−O or C−O−C bending frequency region are downshifted (at ∼530 and ∼552 cm^{-1}), and some new prominent bands appear over the whole spectrum at ∼240, ∼997, ∼1058, ∼1255, 1426, 1499, and 1516 cm^{-1} (Figure 2). A subsequent cycle to lower temperature (163 K) does not lead to any further transformation, as indicated from the Raman bands attributed to the pII phase. This was also recently tested for the 10 mol % H_2CO sample in an X-ray diffraction experiment (see discussion below). One can thus assume that the transformation pI to pII is irreversible and that the thermal treatment applied here certainly favors the stability of pII to the detriment of pI. Due to the high freezing rate, some kinetic effects certainly hinder the formation of pII during the first cooling sequence.

Upon further warming above 233 K, pII begins to melt and transforms into liquid mixtures of oligomers and water molecules. This is clearly evidenced by the presence, in the Raman spectrum, of broad bands similar to those observed in the liquid state and already present at 233 K during the cooling sequence. The melting of remaining ice causes the characteristic low-frequency ice bands to disappear above ∼258 K for the 10 mol % H_2CO sample.

The same general spectroscopic features have been observed for all the concentrations studied: 0.1, 5, 7, 10, 15, and 20 mol % of H_2CO in water. However, it should be mentioned that crystallization kinetics depends on the concentration of the mixtures. For solutions of high concentrations (20 or even 25 mol % H_2CO), the crystallization already takes place during the first cooling at 233 K. This is indicated by the emergence of a pronounced sharp peak at ∼930 cm^{-1} ascribed to C−O stretching (see discussion). Note that solutions of lower concentrations may also crystallize during the freezing sequence from 233 to 163 K, if the kinetics of cooling is sufficiently slow or if an intermediate step (e.g., at 193 K) is added.

IV. Discussion

For a system cooled under extreme nonequilibrium conditions, fast cooling leads generally to incomplete crystallization, and the interrupted crystallization process may continue during rewarming.[25] This phenomenon is generally accompanied by a phase separation that leads to the formation of grains made of

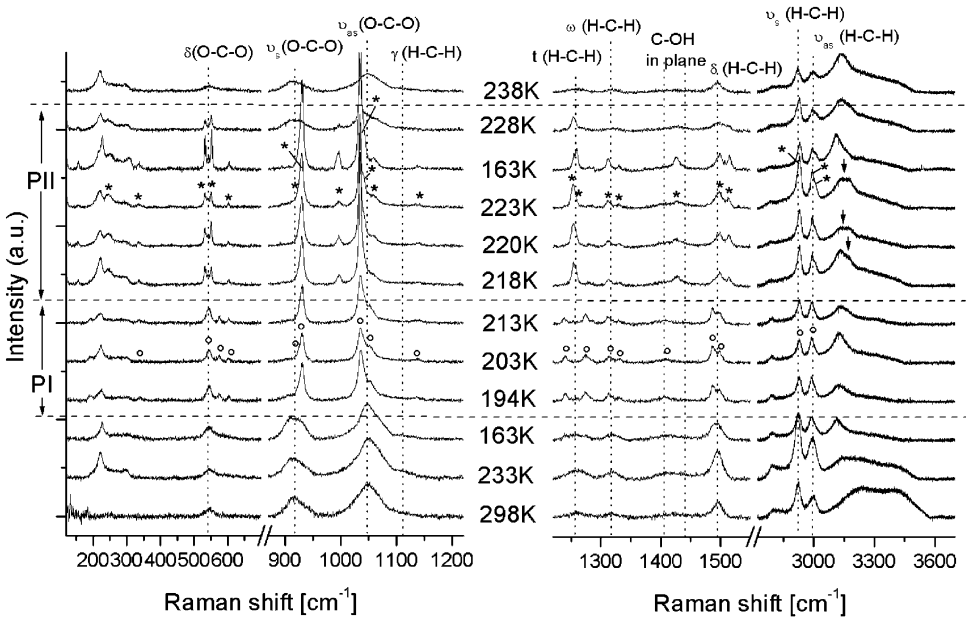

Figure 2. Raman spectra of a frozen aqueous solution containing 10 mol % H_2CO at various temperatures. The spectra cover the frequency range 120−3700 cm^{-1}. The temperature cycle applied should be read from the bottom to the top of the figure. Arrows highlight the characteristic changes of the symmetric O−H stretching (see discussion). Asterisks (*) indicate the characteristic bands for phase pII. Small circles (°) indicate the characteristic bands for phase pI. The position (and attribution) of the vertical dotted lines indicate the band position and the corresponding modes in the liquid aqueous solutions (See ref 16).

TABLE 1: Wavenumbers and Assignments of the Raman Bands in Different Formaldehyde-Based Compounds[a]

phase I		phase II		solid POM (calcd[27])		solid POM (obs)	H_2CO gas		aqueous solution	
ν (cm^{-1})	assignment	ν (cm^{-1})	assignment	ν (cm^{-1})	assignment	(this work) ν (cm^{-1})	ν (cm^{-1})	assignment	ν (cm^{-1})	assignment
		240								
336		336								
545	δ_1	530	δ_1	483	δ_1(COC)				543	δ(OCO)
575	δ_2	552	δ_2	587	δ_2(COC)	536				
603 (w)	δ_3	604 (w)	δ_3	634	δ_3(OCO)	631				
		770 (w)								
910 (w)	ν_{s1}(COC)	912 (w)	ν_{s1}(COC)	916	ν_{s1}(COC)	918 (s)	1746	ν_s(CO)	910	ν_{s1}(OCO)
930	ν_{s2}(COC)	930	ν_{s2}(COC)	930	ν_{s2}(COC)	933			933	ν_{s2}(OCO)
		997								
1036	ν_{as1}(COC)	1035	ν_{as1}(COC)			1038			1040	ν_{as1}(OCO)
1053 (w)	ν_{as2}(COC)	1042 (w)	ν_{as2}(COC)	1072	ν_{as2}(COC)	1091 (s)			1059	ν_{as2}(OCO)
		1058 (w)								
1131 (w)	γ(HCH)	1139 (w)	γ(HCH)	1169	γ(HCH)	1293	1167	γ(HCH)	1111	γ(HCH)
1241	t_1(HCH)	1255	t_1(HCH)							
1275	t_2(HCH)	1260	t_2(HCH)							
1314	ω(HCH)	1313	ω(HCH)	1318	t_1(HCH)	1337			1257	t(HCH)
1330 (w)	ω(HCH)	1330	ω(HCH)	1330	t_2(HCH)	1388				
							1249	ω(HCH)	1315	ω(HCH)
				1407	ω_1(HCH)					
1409	COH in plane	1426	COH in plane	1425	ω_2(HCH)	1437			1408	COH in plane
									1440	
1487	δ_1(HCH)	1499	δ_1(HCH)	1506	δ_1(HCH)	1492	1500	δ(HCH)	1492	δ(HCH)
1498	δ_2(HCH)	1516	δ_2(HCH)	1508	δ_2(HCH)					
2925	ν_s(HCH)	2927	ν_s(HCH)	2924	ν_{s1}(HCH)	2922	2783	ν_s(HCH)	2919	ν_s(HCH)
				2926	ν_{s2}(HCH)					
2992	ν_{as}(HCH)	2992	ν_{as}(HCH)	2977	ν_{as1}(HCH)	2950	2843	ν_{as}(HCH)	2991	ν_{as}(HCH)
		3007		2982	ν_{as2}(HCH)	2994				

[a] The wavenumbers reported for phases pI and pII (see text) correspond to the 10 mol % H_2CO sample at 203 K (pI) and 223 K (pII), respectively. The assignments given for the pI and pII phases are only approximate. Raman wavenumbers and assignments for solid POM are calculated using normal mode analysis.[27] The observed Raman wavenumbers for paraformaldehyde are determined by the least-squares method. Gaseous H_2CO Raman frequencies and assignments are from refs 12 and 28. The Raman wavenumbers given for the aqueous solutions are taken from ref 16. (w) indicates a band of weak intensity; (s) corresponds to a band of strong intensity.

the individual components of the system. At least for low concentrations (≤15 mol % H_2CO), ice is found to crystallize first (Figure 2), and the remaining liquid water mixture is expected to be considerably enriched in oligomers formed in the original liquid solution. The majority of oligomers present in solution will in this case be rejected at the water−ice interface during ice growth and will remain localized at the ice grain boundaries. Additionally, as ice crystallizes, the solute concentration increases in the unfrozen liquid mixture, and one cannot exclude further polymerization reactions from occurring. The degree of polymerization (i.e., the chain lengths of the oligomers) may, therefore, be higher than that of the original aqueous

solution. Incomplete polymerization may happen if the required quantity of water molecules is lacking to maintain an active polymerization process.[15] This may result in the presence of local areas constituted of a mixture of oligomers having various chain lengths, as is the case for aqueous solution with a high H_2CO concentration.[18] Our recent infrared laser resonant desorption work performed on formaldehyde−ice mixtures suggests that short oligomers (also present in the original solutions) remain after quenching at 77 K, as revealed by the low abundance of mixed cluster series such as $(HCO)^+(H_2CO)_p(H_2O)_n$ limited to $p \leq 4$.[24] However, the specific protocol of our Raman experiment provides a different thermal history, which may lead to local areas of heterogeneous concentration where oligomers of various degrees of polymerization are present and different from the original solution. Consequently, the Raman spectroscopic signature will be close to that of a solid mainly composed of monomers and dimers; however, the presence of higher oligomers and water molecules in this crystal cannot be completely ruled out.

To our knowledge, band positions and assignments have only been reported for solid POM, pure gaseous H_2CO, and aqueous formaldehyde solutions[16,27,28] (see Table 1). This may help us in assigning the different bands observed in spectra of the formaldehyde−ice system. The assignment of the bands will be discussed in three frequency regions corresponding to the vibrational modes (deformation and stretching) of CO, CH, and OH groups.

A. C−O Vibrational Mode Spectral Region. As pI crystallizes, the characteristic broad band centered at 543 cm^{-1} in the liquid splits into distinct components at ∼545, 575, and ∼603 cm^{-1} (weak band) (Table 1). This spectral region corresponds to the bending mode. From 213 to 223 K, changes occur with the emergence of peaks at ∼530, ∼552, and ∼604 cm^{-1}, while the bands related to pI disappear completely at 223 K. As reported in Table 1, none of the observed frequencies matches the ones observed or calculated for the solid POM; however, the comparison is not straightforward because the situation in pI or pII is certainly complicated by the contribution of various oligomers with different chain lengths and prevents us at the moment from making a definitive attribution. A theoretical treatment that could help for this assignment is underway in our group.[29] Nevertheless, some insight can be gained on the basis of the previous theoretical treatment of Tadokoro et al.[27] For solid POM, one of the bending modes is affected by the contribution of the γ(HCH) mode (∼24%). This mode is significantly red-shifted, as compared to the other δ(C−O−C) bending modes on using deuterated POM.[27] As a consequence, it was emphasized that this mode constitutes a probe that is sensitive to hydrogen motions. Given the presumably close similarities of a C−O−C chain unit, one can expect the deformation modes of pI or pII to be also sensitive to hydrogen motions. Our preliminary ab initio calculations support this assumption because the vibrational features that characterize the interactions between monomers (methylene glycol), dimers (dioxymethylene glycol), and water molecules suggest a strong contribution from end-chain atoms (i.e., hydrogen) in the bending spectral region.[29] In most cases, the modes in which hydrogen atoms are involved are coupled with the C−O−C or O−C−O bending and lead generally to rocking motions of C−O−H and H−C−H groups. Changes in the frequencies of the bending bands should at least partially be indicative of a modification of the interaction between the oligomers where hydrogen atoms are involved or between oligomers and water molecules. Moreover, intermolecular interactions can be modified by specific arrangements of oligomers in different crystalline structures. Actually, the structural changes with temperature detected by Raman spectroscopy have been confirmed by X-ray diffraction measurements.[30] The emergence of new bands corresponding to the bending modes may, thus, be related to a structural transformation. A distinct phase (pII) is expected to be present with ice above ∼215 K, which is in agreement with the optical observation made (see Figure 1). It should also be noted that within the range 163−213 K, a band is sometimes observed at ∼535 cm^{-1}. Its intensity is comparable to the bands corresponding to the bending modes observed in pI. Furthermore, the spectrum also shows a band at ∼1281 cm^{-1}, especially for mixtures of low concentration (≤ 7 mol % H_2CO). One possible assumption to explain this phenomenon is the formation of a transient phase pIII; however, no definitive conclusion can be made due to the lack of reproducibility of this effect. Hence, we will further focus our discussion on the most often encountered phases pI and pII.

In comparison, the frequencies of the bands ascribed to ν_s(COC) and ν_{as}(COC) C−O stretching modes are slightly affected by the structural transformation (see Table 1). The most significant evolution concerns the C−O bandwidth, which decreases considerably from ∼45 cm^{-1} in the liquid to ∼15 cm^{-1} in the crystal. Two bands at 910 and 933 cm^{-1} assigned to symmetric C−O stretching modes and two other bands at 1040 and 1059 cm^{-1} assigned to antisymmetric C−O stretching modes have been related to intra- and end-chain stretching modes in the aqueous solutions.[16] In the pI phase, a band of high intensity is observed at ∼930 cm^{-1} with a shoulder at ∼910 cm^{-1}. These bands are, thus, related to a symmetric C−O stretching mode. A band of high intensity at ∼1035 cm^{-1} is also observed in pI with a shoulder at ∼1042 cm^{-1} and a weak band at ∼1058 cm^{-1}. These bands can be assigned to antisymmetric C−O stretching modes. The attribution of these modes to intra and end-chain stretching in the crystal is, however, not straightforward and should be considered with caution. The bands corresponding to the symmetric C−O stretching modes at ∼918 cm^{-1} in the solid POM are only slightly shifted when compared to pI and pII (Table 1). On the other hand, for the solid POM, the most intense band of the antisymmetric C−O stretching mode at ∼1091 cm^{-1} is absent in pI and pII. Nevertheless, the band observed at ∼1038 cm^{-1} for the solid POM is assigned to antisymmetric C−O stretching mode according to our preliminary calculations.[29] This band is apparently present in pI and pII and slightly downshifted, which suggests for these phases a similar assignment. Moreover, the crystallization and particular crystallite orientations could change the intensity of some bands that correspond to symmetric vibrational modes. This certainly complicates even more the assignment of the bands corresponding to different C−O modes. A precise assignment should require the knowledge of the crystallographic structure of both phases.

As pII crystallizes, a new band appears at ∼997 cm^{-1}, while the ones assigned to antisymmetric stretching exhibit a complicated underlying fine structure. This last observation may well be correlated with the structural pI−pII phase transformation, since different intermolecular interactions are expected to occur within the different crystalline structures.

B. C−H Vibrational Mode Spectral Region. The bands assigned to δ(H−C−H) CH_2 deformation modes are observed in the region ∼1492 cm^{-1} for the aqueous solutions (Figure 2).[16] As pI crystallizes, two components can be distinguished at 1487 and 1498 cm^{-1} after deconvolution (Table 1). This splitting may result from the different intermolecular interactions

between oligomers in the solid phase. As pII crystallizes, the splitting increases, and the bands are significantly shifted to higher frequencies at ∼1499 and ∼1516 cm^{-1}. This is presumably due to a different structural arrangement (and thus, different interactions) of the oligomers in the pII phase. However, for both the pI and pII phases, the two bands at ∼2927 and ∼2992 cm^{-1} assigned to, respectively, the symmetric and antisymmetric C−H stretching modes, prove in turn to be rather independent of the environment. Moreover, for the pII phase, a shoulder appears at ∼3010 cm^{-1} on the high-frequency side of the band assigned to the antisymmetric C−H stretching mode (Figure 2). This may result from different contributions involving overtones and combination bands.[31] It could also reflect the existence of strong intermolecular interactions between the peripheral hydrogen atoms and the surrounding oligomers or water molecules. Actually, all of these contributions prevent us from giving a precise explanation of all the observed phenomena. The spectral region of twist, wag, and C−O−H in-plane deformation is affected by the crystallization of pI. Weak bands emerge at ∼1241, ∼1275, ∼1314, ∼1330, and ∼1409 cm^{-1} (Table 1). As the pI−pII structural transformation occurs, two strong bands at ∼1255 and ∼1426 cm^{-1} appear along with a weak band at ∼1260 cm^{-1}, while the other two weak bands around 1313 and 1330 cm^{-1} stay unchanged. In comparison, in the aqueous solution, the bands assigned to twisting and wagging motions are found at ∼1257 and ∼1315 cm^{-1}, respectively. Crystallization of the liquid aqueous mixture results apparently in a splitting of the bands assigned to twisting modes at ∼1241 and ∼1275 cm^{-1} in pI and ∼1255 and ∼1260 cm^{-1} in pII. Furthermore, the band located at ∼1315 cm^{-1} splits into two bands at ∼1314 and ∼1330 cm^{-1} assigned to wagging motions in both pI and pII. This effect may result from specific interactions in the solid phases. An important fact is that the bands corresponding to twisting modes are observed and calculated[29] at lower frequencies than those corresponding to the wagging modes in both pI and pII. This feature also applies for the aqueous solutions and for the solid POM, although the bands assigned to twisting and wagging motions are observed at relatively higher frequencies, as compared to those observed for pI and pII phases (Table 1). Assuming a similar origin for the bands at ∼1409 cm^{-1} in pI and ∼1426 cm^{-1} in pII, these bands can well correspond to δ(C−O−H) bending modes involving end-chain atoms. Indeed, the shift observed between these bands (∼17 cm^{-1}) is consistent with a structural change (pI-pII) that affects intermolecular interactions between end-chain units. Finally, the band at ∼1111 cm^{-1} for the aqueous solutions[16] is assigned to the rocking mode (γ(H−C−H)). This band is apparently slightly shifted for the pI and pII phases to ∼1131 and ∼1139 cm^{-1}, respectively (Table 1). However, due to the weak intensity of these bands, their positions are here approximate.

C. Temperature and Concentration Effects on O−H and OH···O Vibrational Modes. In the liquid solutions, since the water is the solvent, the intensity of the bands at ∼3400 cm^{-1} corresponding to O−H stretching modes mainly reflects the contribution from water molecules. Moreover, both symmetric and antisymmetric O−H modes are known to be sensitive to intermolecular interactions.

During the ice formation, the two bands corresponding to these modes are shifted toward lower frequencies (Figure 2) and transform into a band of asymmetric shape. The low-frequency part of this band with high intensity is known to correspond to a mode predominantly of symmetric character (ν_{OH}), while the broad asymmetric part at higher wavenumbers

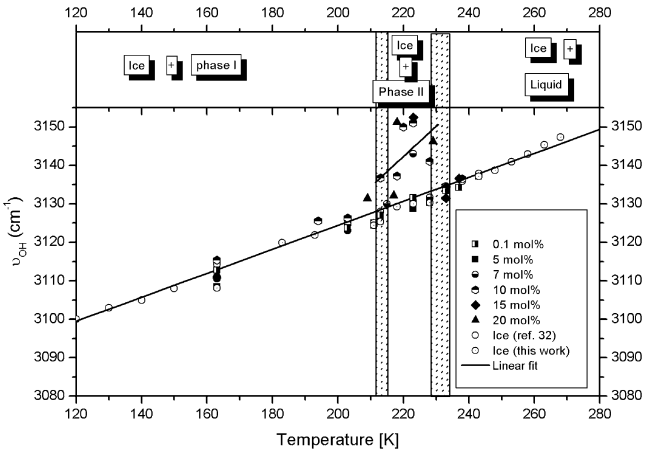

Figure 3. Temperature dependence of the ν_{OH} symmetric stretching of pure ice and frozen ice mixtures with various H_2CO concentration (see text in the inset). The vertical hatched bands indicate the approximate temperature of the pI−pII phase transformation at ∼215 K and the melting of pII at ∼234 K. For the ice and the low concentration ice mixtures, a linear increase of ν_{OH} frequency is observed with temperature (see text). As the structural transformation of pI−pII occurs, there is a clear deviation from linearity for mixtures of high concentration (≥7 mol % H_2CO). In this temperature range and for mixtures of high concentration, the line is drawn as a guide to the eye only. The top of the figure shows the domain of existence of the different phases.

with lower intensity is assigned to mixed modes involving mainly antisymmetric stretching modes (ν_{aOH}).[32] In the following, we will only examine the change with temperature of the OH band corresponding to the symmetric stretching mode (ν_{OH}) for both the pure polycrystalline ice and frozen ice−formaldehyde mixtures (see Figure 3).

For pure ice, ν_{OH} increases with temperature, in agreement with several previous investigations.[32,33] This shift is generally attributed to a volume increase with temperature and reflects partially the decreasing strength of the H-bonds as temperature increases. Other coupled effects concerning intermolecular coupling, anharmonicity of the bonded water molecules, and the geometry of the H-bonds have also to be considered.[34] The rate of change in frequency of ν_{OH} with temperature at constant pressure $(\partial\nu_{OH}/\partial T)_P = -0.31$ cm^{-1} K^{-1} for polycrystalline ice is found to be in reasonable agreement with literature values.[33] To a good approximation, the rate of change of frequency of ν_{OH} calculated over the temperature range 163−223 K for solutions of low concentration (≤5 mol % H_2CO) is found to be similar: $(\partial\nu_{OH}/\partial T)_P = -0.34$ cm^{-1} K^{-1}. In contrast, for solutions of higher concentration (above 5 mol % H_2CO), pronounced concentration effects can be monitored (Figure 3), and an abrupt increase of the OH band frequency arises at the temperature of the pI−pII structural transformation ($T \sim 215$ K). Nonlinear effects in the OH band displacement, as shown in Figure 3, are consistent with a structural rearrangement in the crystal. Indeed, it is conceivable that such structural changes induce the formation of H-bonds between the oligomers and water molecules. If nonequivalent OH···O distances (different from those in ice) between water molecules and oligomers arise, this will cause variations in the H-bonds' strength and, thus, of the ν_{OH} stretching frequencies (Figure 3). Similar effects have already been observed for ice polymorphs in which nonequivalent H-bond lengths exist in the different structures.[35,36] From the blue-shifted ν_{OH} value for the pII phase (∼20 cm^{-1}, Figure 3), one can expect that weaker H-bonds have formed between water molecules and oligomers, as compared to those existing in ice. Additional effects that may contribute to the ν_{OH} shift

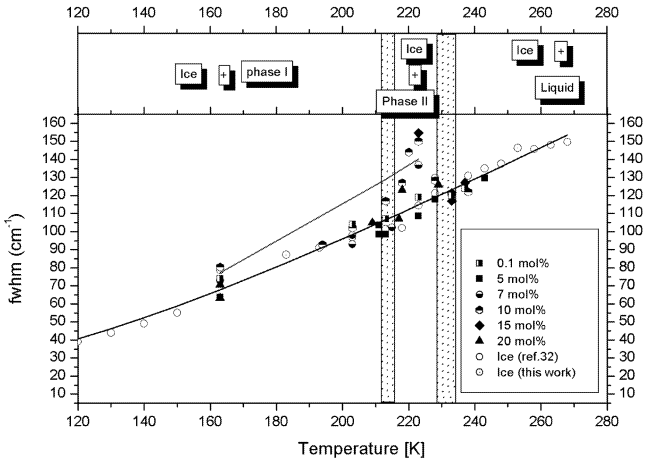

Figure 4. Temperature dependence of the bandwidth (fwhm) of the ν_{OH} symmetric stretching mode of pure ice and frozen ice mixtures with various H_2CO concentrations (see text in the inset). The vertical hatched bands indicate the approximate temperature of the pI−pII phase transformation at ∼215 K, and the melting of pII at ∼234 K. The lines are drawn as a guide to the eye only. The top of the figure shows the domain of existence of the different phases.

are the different conformations that the oligomer chains may adopt within the structure.[27,37] This may tend to distort the H-bonds' geometry. Such contribution applied in icelike structures or other ice polymorphs.[36,38,39] Likewise, a strong intermolecular coupling of the O−H oscillators as well as the anharmonicity of the intramolecular O−H oscillators may account for the ν_{OH} frequency shift with temperature.[34] With the aforementioned coupled effects on the O−H stretching frequency in the formaldehyde−ice mixtures, it is, at evidence, difficult to say which contribution prevails without using an isotopic dilution method. This will be the focus of a future work.

In the temperature domain where ice and pI coexist, no significant deviation compared to the pure ice linear behavior is observed, whatever the concentration is. This suggests that the oligomers interact through relatively weaker intermolecular forces (presumably van der Waals or weak H-bonds) with the surrounding water molecules in the structure pI. Our results may support the assumptions of Kosevich et al.[23] on the existence of weak van der Waals forces between ice and the oligomers. However, one has to assume that their concentrated (40% H_2CO) quenched solutions at 77 K result either in the formation of pI or in an unfrozen liquid water−oligomer state or in a combination of both, as observed here. Further comparison with their work is difficult because their sample may be strongly affected by the presence of methanol (10−15%), usually added as a stabilizer in concentrated commercial solution.[28]

Also related to the ν_{OH} frequency shift is the surprising increase in the bandwidth (fwhm) throughout the temperature range of the existence of pII, between ∼218 and 223 K (Figure 4). An increase in the bandwidth with increasing temperature is generally associated with an increase in the vibrational amplitudes of the atoms about their equilibrium positions due to thermal smearing.[40] Additionally, both intermolecular coupling and a distribution of the OH···O bond lengths due to proton disorder in ice may also contribute to a band broadening.[32] As suggested above, spatial effects will also certainly be enhanced if nonequivalent H-bonds are formed between water molecules and oligomers.

Further evidence of the formation of hydrogen bonds for pII is the emergence of low-frequency bands (the most intensive being at ∼240 cm^{-1}, Figure 2). This is generally a characteristic spectral change brought about by H-bond formation in a wide variety of liquid and solid phases[41] in which OH···O stretching and O−H···O bending modes are thought to be involved, as in H-bonded solids.[42] Additionally, nonequivalent H-bonds, as those proposed in structure pII, may partially induce such effects and correlatively enrich the low-frequency part of the spectrum corresponding to lattice modes, as observed in ice polymorphs or hydrates.[43] Thus, the 240 cm^{-1} band may be assigned to the translational mode of water molecules H-bonded to oligomers. As a consequence, the rate of change in frequency of the band assigned to the translational mode ν_T (at ∼220 cm^{-1}) in ice cannot especially be used to characterize either the pI or pII phase.

V. Summary

Raman spectroscopy proves to be a very useful and sensitive nondestructive method to investigate the effects of freezing on the water−formaldehyde system for different concentrations and to establish related information on ice−formaldehyde interactions. Upon freezing at a relatively low rate (∼40 K/min), solutions of low concentration (≤15 mol % H_2CO) are unable to completely crystallize unless the cooling is slowed and additional steps at intermediate temperatures are added. On the other hand, crystallization is readily initiated during the applied cooling sequence for the mixture of highest concentration (20 mol % H_2CO). During the heating sequence, the system almost completely crystallizes into ice and a phase pI at any concentration. A small amount of a residual unfrozen liquid, however, is found to coexist with ice and the phase pI. This unfrozen liquid is heterogeneously dispersed throughout the sample surface and presumably mainly composed of concentrated oligomers. Subtle changes happen for the bands assigned to the C−O stretching and bending modes of the oligomers as the temperature reaches ∼218 K. These bands are sensitive to the oligomer−water interactions. The observed changes can be related to a structural transformation with the emergence of a distinct crystalline phase (pII) apparently stable over the whole temperature range explored, 163−234 K. C−H vibrational modes are also sensitive to the crystallization and the structural transformation, as revealed by changes in the bands assigned to bending H−C−H modes. For the pII phase, the temperature dependency of the frequencies and width of the bands assigned to the O−H stretching modes of water molecules suggests the existence of strong interactions between the oligomers and water molecules. It is, thus, expected that the crystalline pII phase is built with a hydrogen-bonded network composed of oligomers and water molecules having nonequivalent OH···O bonds. In contrast, it is expected that weak interactions (presumably van der Waals or weak H-bonds) occur between oligomers present in pI and water molecules of the remaining unfrozen liquid mixture or the surrounding ice (assuming pI is mainly composed of oligomer species).

Further investigations are in progress to relate our Raman measurements to crystallographic and thermodynamic work to give a complete picture of the formaldehyde−ice system at temperatures below freezing. Results of this work are of major interest in cryospheric sciences. It also highlights the complexity of the mechanism that may take place in cryobiological systems during freeze−thaw cycles when organic and biological molecules interact with water. An important perspective of our future work concerns gas mixtures of current interest in systems ranging from Earth's atmosphere to interstellar clouds or comets. In these contexts, solid ice mixtures often result from gas condensation instead of freezing of liquid mixtures. The characterization and identification of solid phases formed under

such conditions require synthesis in well-controlled pressure, temperature, and composition conditions and represent a challenging task. This can be addressed by laboratory and simulation studies that are necessary to quantify processes relevant to astrophysics and atmospheric chemistry. For example, the perturbation of the ice structure by doping species, the formation of hydrate phases, and the ability of gases to diffuse into the ice lattice may have a strong influence on the efficiency of heterogeneous (induced) reactions. Therefore, information related to the composition, the structural arrangements, and the formation temperature of ice−gas mixtures can help in the understanding of the removal of trapped gases and the redistribution of reactive chemical species in the environment.

Acknowledgment. The Centre d'Etudes et de Recherches Lasers et Applications is supported by the Ministère Chargé de la Recherche, the Région Nord−Pas de Calais, and the Fonds Européen de Développement Economique des Régions. This research is partially supported by the Groupement de Recherche "Réactivité à la Surface de la Glace" and the "Programme National de Chimie Atmosphérique" (PNCA) of the Centre National de la Recherche Scientifique. D. Prevost is gratefully acknowledged for his help during the experimental sample preparation. We also thank M. Ziskind and C. Mihesan for helpful discussions.

References and Notes

(1) Dominé, F.; Shepson, P. B. *Science* **2002**, *297*, 1506.
(2) Foster, K. L.; Plastridge, R. A.; Bottenheim, J. W.; Shepson, P. B.; Finlayson-Pitts, B. J.; Spicer, C. W. *Science* **2001**, *291*, 471.
(3) Sumner, A. L.; Shepson, P. B. *Nature* **1999**, *398*, 230.
(4) Fan, Q.; Dasgupta, P. K. *Anal. Chem.* **1994**, *66*, 551.
(5) Crutzen, P. J.; Fishman, J. *Geophys. Res. Lett.* **1977**, *4*, 321.
(6) Staffelbach, T.; Neftel, A.; Stauffer, B.; Jacob, D. *Nature* **1991**, *349*, 603.
(7) Huebner, W. F. *Science* **1987**, *237*, 628.
(8) Mitchell, D. L.; Lin, R. P.; Anderson, K. A.; Carlsson, C. W.; Curtis, D. W.; Korth, A.; Rème, H.; Sauvaud, J. A.; d'Uston, C.; Mendis, D. A. *Science* **1987**, *237*, 626.
(9) Sumner, A. L.; Shepson, P. B.; Grannas, A. M.; Bottenheim, J. W.; Anlauf, K. G.; Worthy, D.; Schroeder, W. H.; Steffen, A.; Dominé, F.; Perrier, S.; Houdier, S. *Atmos. Environ.* **2002**, *36*, 2553.
(10) Mumma, M. J.; Reuter, D. C. *Astrophys. J.* **1999**, *344*, 940.
(11) Allamandola, L. J.; Sandford, S. A.; Valero, G. J. *Icarus* **1988**, *76*, 225.
(12) Schutte, W. A.; Allamandola, L. J.; Sandford, S. A. *Icarus* **1993**, *104*, 118.
(13) Schutte, W. A.; Allamandola, L. J.; Sandford, S. A. *Adv. Space Res.* **1995**, *15*, 401.
(14) Schutte, W. A.; Allamandola, L. J.; Sandford, S. A. *Science* **1993**, *259*, 1143.
(15) Le Botlan, D. J.; Mechin, B. G.; Martin, G. J. *Anal. Chem.* **1983**, *55*, 587.
(16) Lebrun, N.; Dhamelincourt, P.; Focsa, C.; Chazallon, B.; Destombes, J. L.; Prevost, D. *J. Raman Spectrosc.* **2003**, *34*, 459.
(17) Spence, R.; Wild, W. *J. Chem. Soc.* **1935**, 506.
(18) Walker, J. F. *Formaldehyde*; American Chemical Society Monograph Series: New York, 1964.
(19) Franks, F. In *Water. A Comprehensive Treatise*; Franks, F., Ed;, Plenum Press: London, 1983; Vol. 7, Chapter 4.
(20) Mazur, P. *Science* **1970**, *168*, 939.
(21) Skaer, H. le B.; Franks, F.; Echlin, P. *Cryobiology* **1978**, *15*, 589.
(22) Morris, G. J.; Clarke, A. *Effects of Low Temperature on Biological Membranes*; Academic Press: London, 1981.
(23) Kosevich, M. V.; Boryak, O. A.; Shelkovsky, V. S.; Derrick, P. J. *Eur. Mass Spectrom.* **1998**, *4*, 31.
(24) Mihesan, C.; Lebrun, N.; Ziskind, M.; Chazallon, B.; Focsa, C.; Destombes, J. L. *Surf. Sci.* **2004**, *566−568*, 650.
(25) Luyet, B. *Proc. N. Y. Acad. Sci.* **1965**, *125*, 502.
(26) Faure, P.; Chosson, A. *J. Glaciol.* **1978**, *21*, 65.
(27) Tadokoro, H.; Kobayashi, M.; Kawaguchi, Y.; Kobayashi, A.; Murahashi, S. *J. Chem. Phys.* **1963**, *38*, 703.
(28) Möhlmann, G. R. *J. Raman Spectrosc.* **1987**, *18*, 199.
(29) Toubin, C. et al., in preparation.
(30) Lebrun, N. et al., in preparation.
(31) Colthup, N. B.; Daly, L. H.; Wiberley, S. E. *Introduction to infrared and Raman spectroscopy*, 3rd edition; Academic Press: New York, 1990.
(32) Sivakumar, T. C.; Rice, S. A.; Sceats, M. G. *J. Chem. Phys.* **1978**, *69*, 3468.
(33) Bertie, J. E.; Labbé, H. J.; Whalley, E. *J. Chem. Phys.* **1969**, *50*, 4501.
(34) Johari, G. P.; Chew, H. A. M. *Philos. Mag. B* **1984**, *49*, 647.
(35) Bertie, J. E.; Whalley, E. *J. Chem. Phys.* **1964**, *40*, 1646.
(36) Minceva-Sukarova, B.; Sherman, W. F.; Wilkinson, G. R. *J. Phys. C: Solid State Phys.* **1984**, *17*, 5833.
(37) Carazzolo, G.; Mammi, M. *J. Polym. Sci. Part A: Polym Chem.* **1963**, *1*, 965.
(38) Johari, G. P.; Chew, G. P. *Nature* **1983**, *303*, 604.
(39) Johari, G. P.; Chew, G. P. *Philos. Mag. B* **1984**, *49*, 281.
(40) Turrel, G. *Infrared and Raman Spectra of Crystals*; Academic Press: London, 1972.
(41) Pimentel, G. C.; McCellan, A. L. *The Hydrogen Bond*; Pauling, L., Ed.; W. H. Freeman: San Fransisco, CA, 1960.
(42) Ratajczak, H.; Yaremko, A. M. *Chem. Phys. Lett.* **1999**, *314*, 122.
(43) Bertie, J. E.; Othen, D. A.; Solinas, M. *Physics and Chemistry of Ice*; Whalley, E., Jones, S. J., Gold, I. W., Eds.; , Ottawa, 1973.